Warming of the Arctic lower stratosphere by light absorbing particles

D. Baumgardner,[1] G. Kok,[1,2] and G. Raga[1]

Received 20 October 2003; revised 29 January 2004; accepted 24 February 2004; published 24 March 2004.

[1] Recent measurements of light absorbing particles in the Arctic lower stratosphere show significantly higher mass concentrations of black carbon than were measured in 1992. The difference is primarily a result of measurements with a more quantitative and accurate technique than was previously used. We attribute the large amount of light absorbing material to transport from lower latitude, tropospheric sources rather than increases in aircraft emissions. The calculated heating rate in this aerosol layer, as compared to an atmosphere consisting of only gases, increases by 12% during the winter. This is a result of light absorption by the particles and could perturb the altitude of the local tropopause and affect tropospheric/stratospheric exchange processes. *INDEX TERMS:* 0305 Atmospheric Composition and Structure: Aerosols and particles (0345, 4801); 0322 Atmospheric Composition and Structure: Constituent sources and sinks; 0394 Atmospheric Composition and Structure: Instruments and techniques. **Citation:** Baumgardner, D., G. Kok, and G. Raga (2004), Warming of the Arctic lower stratosphere by light absorbing particles, *Geophys. Res. Lett.*, *31*, L06117, doi:10.1029/2003GL018883.

1. Background

[2] Light absorption by soot and dust particles change the thermodynamic structure of the atmosphere and contribute to regional and global climate change [*Hansen et al.*, 1980; *Turco et al.*, 1990; *Charlson et al.*, 1992; *Penner et al.*, 1992]. The lower stratosphere is particularly sensitive to the presence of light absorbing particles (LAP) since they can reside from months to years, in contrast with upper tropospheric lifetimes of days to weeks. The source of these particles may be aircraft [*Pueschel et al.*, 1992, 1997; *Blake and Kato*, 1995; *Rahmes et al.*, 1998; *Strawa et al.*, 1999], meteorites [*Murphy et al.*, 1998] or transport from tropospheric sources [*Cook and Wilson*, 1996; *Liousse et al.*, 1996; J. Hendricks et al., Simulating the global atmospheric black carbon cycle: A revisit to the contribution of aircraft emissions, submitted to *Atmospheric Chemistry and Physics*, 2004, hereinafter referred to as Hendricks et al., submitted manuscript, 2004]. A serious dearth of accurate and quantitative measurements limits our understanding of the origin and lifetime of these types of particles and their impact on climate. Here we present measurements of LAP in the Arctic lower stratosphere made with a new instrument, the single particle soot photometer (SP2).

2. Measurement Methods

[3] The SP2 uses a patented technique [*Stephens et al.*, 2003] that combines the principles of light scattering, absorption and emission to derive the diameter, mass and incandescence temperature of individual aerosol particles in the diameter range from 0.15 to 1 μm. Particles enter the sample cavity of the SP-2 from an isokinetic inlet mounted on the exterior of the aircraft and pass through the beam of a diode-pumped Nd:YAG laser (1.06 μm wavelength) where they scatter or absorb light. Two cones of scattered light, 30°–60° and 120°–150° are collected by the optics and focused on a photodetector that produces a voltage signal proportional to the scattering intensity. Particles that contain light absorbing material, at the wavelength of the laser, are heated as they pass through the beam and reach a temperature at which they incandesce and emit light at a wavelength that is proportional to the incandescence temperature. This emitted light is collected by two separate detectors with filters that select the wavelengths of 350–800 nm and 630–800 nm.

[4] Particle diameter is derived from the scattered light using classical Mie theory [*Mie*, 1908]. The mass of light absorbing material in a particle is linearly proportional to the magnitude of incandescence. Calibration is with commercially available spherical carbon particles of known density and whose specific sizes are selected with an electrostatic classifier. Scattering and incandescence signals from the detectors are related to the particle diameter and mass over a size range from 0.126 μm to 1.0 μm. The temperature of incandescence is calculated from the ratio of signals from the incandescence detectors using Plank's law for black body radiation. The composition of the absorbing material is estimated from the temperature of incandescence, e.g., black carbon (BC) has a temperature of incandescence between 3500 and 4500 K. The estimated uncertainty in derived mass from absorbing particles is ±50%, dependent on the accuracy of calibration, uncertainty in sample volume and possible wall losses in the inlet and tubing. The uncertainty in mass calculated for non-absorbing particles is ±50% as a result of the assumptions used for calculating size from Mie scattering that depend on the refractive index, a value that can only be estimated based upon assumed particle composition. The temperature of incandescence can be derived with an accuracy of ±10%.

[5] An effect called charring is a source of uncertainty in the derivation of LAP mass. This effect has sometimes been observed in the thermal analysis of aerosol-loaded filters that are heated and some organic compounds are converted to BC. This is an effect that will be studied further in a controlled laboratory experiment; however, this effect should not contribute much to the measured BC in the present study as it is unlikely that organic

[1]Centro de Ciencias de la Atmósfera, Universidad Nacional Autónoma de México, Mexico City, Mexico.
[2]Now at Droplet Measurement Technologies, Boulder, Colorado, USA.

0094-8276/04/2003GL018883$05.00

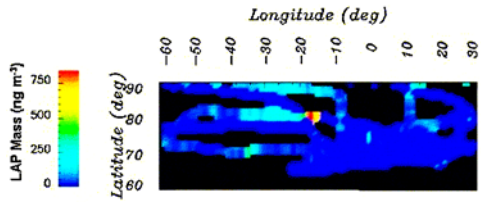

Figure 1. Map of light absorbing particle mass in the Arctic Stratosphere. The coloured regions on this map, compiled from six flights, show average values of LAP mass, in ng m^{-3}. The scale on the left defines the range of values.

layers are a significant component of the stratospheric particles.

3. Results

[6] The SP2 was deployed on the NASA DC-8 research aircraft during the second SAGE III Ozone Loss and Validation Experiment as part of the field campaign based in Kiruna, Sweden (67.8N, 20.3E), to evaluate ozone loss processes in the polar vortex. Most flight tracks were higher than 9 km and within a region bounded by the North Pole and the west coast of Greenland. The following discussion is based on the analysis of measurements made during six flights from January 26–February 4, 2003 and is restricted to periods when the aircraft was above the tropopause, defined by values of ozone that exceed 100 ppb [*Koike et al.*, 2002]. The SP2 measures and stores the scattering and incandescence signals from every particle, but the measurements are averaged in 60-second segments to improve sample statistics. The sample flow was maintained at 2.0 cm^3 s^{-1} and the average number concentration was 1–10 cm^{-3}; hence, approximately 120–1200 particles were analysed during each sample interval, a period that corresponds to a distance of approximately 12 km. The number and mass concentrations reported here are normalized to standard temperature and pressure.

[7] Figure 1 shows the spatial distribution of the average mass concentrations of LAP for all flights, illustrating the wide range in LAP mass concentrations over this region of the Arctic and indicating an increase with latitude. Figure 2 shows this trend where the measurements have been averaged in two-degree intervals of latitude. In the lower panel, the solid line is the average (vertical bars are the standard deviation about the mean) and the dashed line is the maximum mass measured in each latitude interval. As seen in the upper panel (solid line), the LAP particles are 20–60% of the total particle number concentration measured with the SP2. Two condensation nuclei counters (CN) were also sampling from the same inlet as the SP-2. One counter heated the air to 300° prior to measurements in order to remove volatile particles. The dashed line in the upper panel of Figure 2 shows the ratio of heated to non-heated CN concentrations. The trend and magnitude of the non-volatile fraction, i.e., BC, is in good agreement with the LAP fraction. The average LAP mass varies from 0.2–200 ng m^{-3} and the maximum from 1–1000 ng m^{-3}. Particles with incandescence temperatures greater than 3500 K are classified as BC. Those that incandesce at lower temperatures can be certain pure metals, e.g., Al, Fe, and Cu. The frequency diagram of incandescence temperature (Figure 3) shows that ≈60% of the LAP is BC. The distribution by size of these particles is sensitive to their

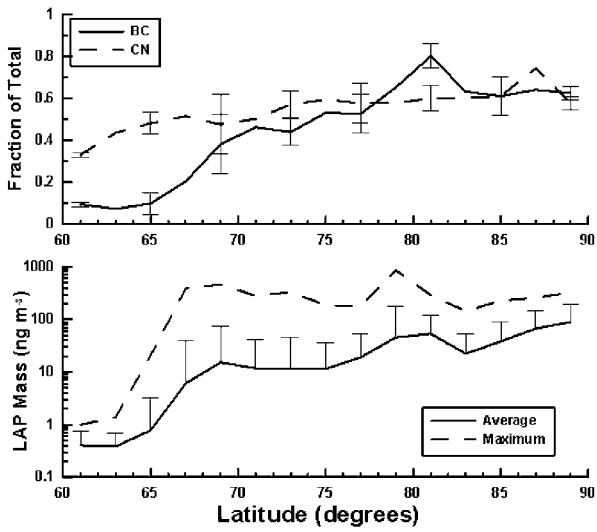

Figure 2. Latitudinal profile of LAP mass (lower panel) and fraction of particles that were LAP or non-volatile particles (upper panel). The LAP mass and number fractions are averaged in 2° intervals using measurements from the six flights over the region displayed in Figure 1. The vertical bars denote the standard deviation about the average in each latitude interval. In the upper panel the LAP fractions (solid) represent the ratio between incandescing and all particles measured with the SP-2. CN fractions (dashed) are the ratio of heated to unheated concentrations.

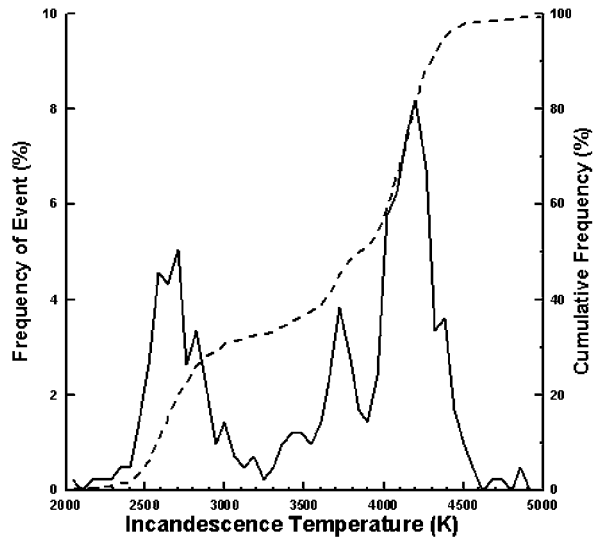

Figure 3. Frequency of incandescence temperatures. Each frequency event represents a 60-second average. Temperatures between 3500 and 4500° K are representative of black carbon, whereas particles with lower incandescence temperatures are possibly Al, Cr, Cu, Fe or Ni.

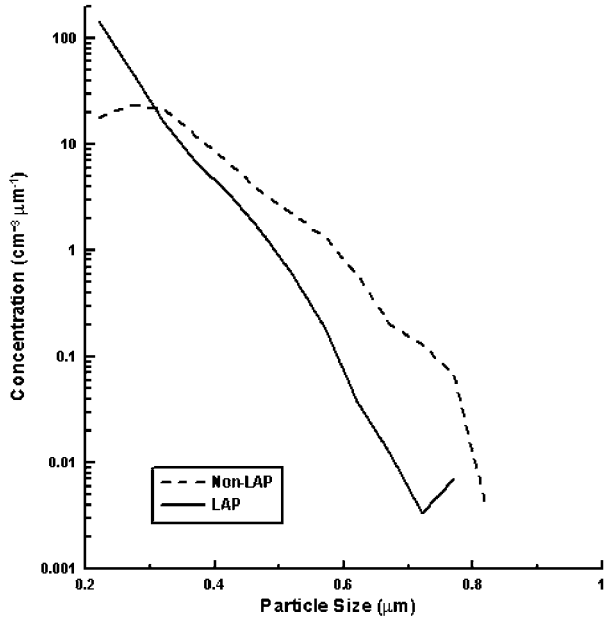

Figure 4. Aerosol size distributions. The number concentration of light absorbing and non-light absorbing particles are presented as a function of estimated diameter to illustrate that LAP dominate the concentration of particles less than 0.3 μm.

composition. There is 10 times more LAP with diameters less than 0.3 μm than non-LAP (Figure 4).

4. Discussion

[8] Comparisons were made between the BC measurements from the 2003 campaign and with measurements made with a different technique but in the same region, during the same season and from the same aircraft in 1989 and 1992 [*Pueschel et al.*, 1992; *Blake and Kato*, 1995; *Pueschel et al.*, 1997]. The previous study measured average BC mass concentrations from 0.08 to 0.4 ng m^{-3} and an average mass fraction of 0.006 [*Blake and Kato*, 1995]. The SP2 measured an average mass concentration of LAP from 0.2 to 200 ng m^{-3} and mass fractions from 0.2 to 0.7. The mass concentrations measured by the SP2 are generally many times greater than those of the 1992 studies. The fraction of particles that contained light absorbing material is 30–100 times larger than previously reported.

[9] The earlier studies used a subjective derivation of BC by visual inspection of particles collected from airborne wire impactors. This technique has an estimated uncertainty of at least ±1000% due to the sampling and methodology used in the analysis [*Blake and Kato*, 1995]. In addition, the analysis can only identify BC that is unmixed with other compounds, and metals and dust were also excluded. Recent measurements [*Murphy et al.*, 1998] show that these latter compounds are frequently found within stratospheric particles.

[10] Aircraft emissions or biomass burning are possible sources for stratospheric BC. The role of aircraft has been investigated in a previous study in which eleven transport models were used to evaluate the global distribution of BC [*Danilin et al.*, 1998]. These models predicted an average maximum BC mass of 0.6 ± 0.5 ng m^{-3}, located between 10 and 12 km at 60°N ± 9° latitude. The basis of these model estimates is the 1992 inventory of fuel consumption by commercial aircraft [*Baughcum et al.*, 1996] and assume a BC emission factor of 0.04. From comparisons with the SP2 measurements we conclude that aircraft emissions are not the primary source of BC in the Arctic stratosphere. However, in the winter when the Arctic vortex is well developed, aircraft emissions might accumulate in this region. We made the majority of measurements within the vortex where the particles have long lifetimes due to the low sedimentation velocity of sub-micron particles (0.01 cm s^{-1}). An analysis of back trajectories for the flights in this study showed that more than 95% of the sampled air parcels had been in the Arctic stratosphere during the previous 10 days. Hence, accumulation of particles in the vortex may be possible from local sources such as aircraft. However, the air in the vortex is generally subsiding, and hence results in the loss of material through the tropopause at the bottom of the polar vortex. Given this removal process, extended calculations beyond the scope of this article are needed to determine if particles are leaving the vortex faster than they are bring produced by local sources and entrainment at the vortex edges.

[11] Emissions from biomass burning and urban combustion, as sources of stratospheric aerosols, have been evaluated with three dimensional, global transport models and suggest that BC from tropospheric sources reach the Artic stratosphere [*Cook and Wilson*, 1996; *Liousse et al.*, 1996]. A recent simulation [Hendricks et al., submitted manuscript, 2004] predicts average BC mass as large as 10 ng m^{-3} at the altitudes and latitudes of measurements made during SOLVE II, but cannot explain the large range of observed values.

[12] Particles modify the flux of solar and infrared radiation, as a function of particle optical properties, i.e., the extinction coefficient, σ_e, the single scattering albedo, ω_o and the asymmetry factor, g. These properties are dependent on particle size, shape and composition and vary with the wavelength of the incident radiation. The region within which the particles reside may be warmed due to the combined effects of scattering and absorption of solar and infrared radiation [*Pollack et al.*, 1981]. Modelling studies [*Lacis et al.*, 1992] have shown that the heating caused by aerosols, depending on the altitude, can increase by almost a factor of 10 when ω_o decreases as little as 5%.

[13] The values σ_e, ω_o and g were computed from the measured size distributions for an incident wavelength of 550 nm, assuming that the non-absorbing component was sulphuric acid [*Pollack et al.*, 1981] with a refractive index appropriate for a 75% solution by weight [*Palmer and Williams*, 1975; *Gandrud and Lazrus*, 1981]. A refractive index of 1.8 −0.5i is used for the LAP [*Twitty and Weinman*, 1971] under the assumption that the majority of these particles are BC.

[14] The average and maximum extinction coefficients, calculated from the measured size distributions between 9 and 12 km, are 4×10^{-5} and 6×10^{-4} km^{-1}. The single scattering albedos for the average and maximum extinctions are 0.92 and 0.73, respectively and the average asymmetry factor is 0.55. This value of g agrees well with the value of

0.49 ± 0.7 that was determined from direct measurements in the stratosphere over Alaska in 1981 [*Grams*, 1981].

[15] The effect of LAP on radiative fluxes was evaluated with a 14 stream radiative transfer model [*Key and Schweiger*, 1998] that incorporates 129 spectral bands from 0.28 μm to 500 μm. A single layer from 9–12 km, with the measured σ_e, ω_o and g, was used to evaluate the effect of the LAP. Standard vertical profiles of temperature, pressure, water vapour, O_3, CO_2 and O_2 were used assuming conditions for a sub-arctic winter (70°N) over a surface with a reflectance corresponding to bare sea ice [*Brieglieb et al.*, 1986; *Ellingson et al.*, 1991; *Tsay et al.*, 1989].

[16] The heating rate was calculated in the 9–12 km layer for gas absorption only and for gases plus LAP, all for a solar zenith angle of 78° (mid-February at 1400 GMT). The layer with only gases cools at a rate of −0.8°C/day and −0.7°C/day with the addition of LAP layer. Thus, the impact of the thin layer of LAP is to offset by 12% the cooling of the atmosphere by gases. This is significant because of the potential impact on the thermodynamic structure of the tropopause. The tropopause is formed by the balance between radiative cooling from gases in the stratosphere and warming by convection from the troposphere [*Holton et al.*, 1995]. A decrease in cooling rate will lead to a higher tropopause. The exchange of material, such as water vapour, ozone, or CFCs, between the stratosphere and troposphere is sensitive to this height of the tropopause [*Holton et al.*, 1995]. The LAP is clearly inhomogeneous, as seen in Figure 1, and the measurements only extend to 12 km. Previous studies with higher altitude aircraft [*Pueschel et al.*, 1997; *Strawa et al.*, 1999] have measured BC at altitudes as high as 20 km, suggesting that the absorbing layer is deeper and the radiative impact is larger than predicted in the current study.

5. Summary

[17] BC mass concentrations in the Arctic vortex between 0.2 and 1000 ng m^{-3} as measured with a new technique. These values are higher than reported by previous studies that used less quantitative techniques. The source of the BC could be a result of accumulated aircraft emissions but is more likely from tropospheric sources.

[18] A large fraction (>40%) of particles have lower incandescence temperatures that are characteristic of a number of pure metals. Since these metals have much higher absorption cross sections than BC, their effect on local heating rates could be significant.

[19] Regardless of their origins, LAP have the potential to significantly perturb climate in the stratospheric polar region. The recent measurements indicate that more BC mass is present in the Arctic stratosphere than previously assumed, but more extensive measurements are required before these results can be extended globally.

[20] **Acknowledgments.** The Office of Naval research funded the development of the SP2, the NASA Radiation Sciences Program funded the participation of the SP2 in SOLVE II and David Fahey provided guidance for comparing the SP2 measurements with predictions from aircraft emission transport models. We thank M. Schoeberl, L. Lait and P. Newman for the back trajectory analysis, M. Avery for the ozone measurements used to differentiate tropospheric and stratospheric air masses and B. Andersen for the volatility measurements.

References

Blake, D. F., and K. Kato (1995), Latitudinal distribution of black carbon soot in the upper troposphere and lower stratosphere, *J. Geophys. Res.*, *100*, 7195–7202.

Baughcum, S. L., et al. (1996), Scheduled civil aircraft emission inventories for 1992: Database development and analysis, *NASA Contract. Rep., NASA CR 4700*, 214 pp.

Brieglieb, B. P., et al. (1986), Comparison of regional clear-sky albedos inferred from satellite observations and model computations, *J. Clim. Appl. Meteorol.*, *25*, 214–226.

Charlson, B. J., et al. (1992), Climate forcing by anthropogenic aerosols, *Science*, *255*, 423–430.

Cook, W. F., and J. N. Wilson (1996), A global black carbon model, *J. Geophys. Res.*, *101*, 19,395–19,409.

Danilin, M. Y., et al. (1998), Aviation fuel tracer simulation: Model intercomparison and implications, *Geophys. Res. Lett.*, *25*, 3947–3950.

Ellingson, R. G., et al. (1991), The intercomparison of radiation codes used in climate models: Long wave results, *J. Geophys. Res.*, *96*, 8929–8953.

Gandrud, B. W., and A. L. Lazrus (1981), Measurements of sulfate mixing ratio with multifilter sampler, *Geophys. Res. Lett.*, *8*, 21–22.

Grams, G. W. (1981), In-situ measurements of scattering phase functions of stratospheric aerosol particles in Alaska during July 1979, *Geophys. Res. Lett.*, *8*, 13–14.

Hansen, J. E., et al. (1980), Climatic effects of atmospheric aerosols, *Ann. N.Y. Acad.*, *338*, 575–587.

Holton, J. R., et al. (1995), Stratosphere-troposphere exchange, *Rev. Geophys.*, *33*, 403–439.

Key, J., and A. J. Schweiger (1998), Tools for atmospheric radiative transfer: Streamer and FluxNet, *Comput. Geosci.*, *24*, 443–451.

Koike, M., et al. (2002), Redistribution of recative nitrogen in the Arctic lower stratosphere in the 1999/2000 winter, *J. Geophys. Res.*, *107*(D20), 8275, doi:10.1029/2001JD001089.

Lacis, A., et al. (1992), Climate forcing by stratospheric aerosols, *Geophys. Res. Lett.*, *19*, 1607–1610.

Liousse, C., et al. (1996), A global three-dimensional model study of carbonaceous aerosols, *J. Geophys. Res.*, *101*, 19,411–19,432.

Mie, G. (1908), Beitrage zur optik trüber medien speziell kolloidaler metallösungen, *Ann. Phys.*, *25*, 377–445.

Murphy, D. M., et al. (1998), In situ measurements of organics, meteoritic material, mercury, and other elements in aerosols at 5 to 19 kilometers, *Science*, *282*, 1664–1669.

Palmer, K. F., and D. Williams (1975), Optical constants of sulfuric acid: Application to the clouds of Venus?, *Appl. Opt.*, *14*, 208–219.

Penner, J. E., et al. (1992), Effects of aerosols from biomass burning on the global radiation budget, *Science*, *256*, 1432–1434.

Pollack, J. B., et al. (1981), Radiative properties of the background stratospheric aerosols and implications for perturbed conditions, *Geophy. Res. Lettr.*, *8*, 26–28.

Pueschel, R. F., et al. (1992), Black carbon (soot) aerosol in the lower stratosphere and upper troposphere, *Geophys. Res. Lett.*, *19*, 1659–1662.

Pueschel, R. F., et al. (1997), Soot aerosol in the lower stratosphere: Pole-to-pole variability and contributions by aircraft, *J. Geophys. Res.*, *102*, 13,113–13,118.

Rahmes, T. F., et al. (1998), Atmospheric distributions of soot particles by current and future aircraft and resulting radiative forcing on climate, *J. Geophys. Res.*, *103*, 31,675–31,667.

Stephens, M., et al. (2003), Particle identification by Laser Induced Incandescence in a solid state laser cavity, *Appl. Opt.*, *42*, 3726–3736.

Strawa, A. W., et al. (1999), Carbonaceous aerosol (soot) measured in the lower stratosphere during POLARIS and its role in stratospheric photochemistry, *J. Geophys. Res.*, *104*, 26,753–26,766.

Tsay, S.-C., et al. (1989), Radiative energy budget in the cloudy and hazy Arctic, *J. Atmos. Sci.*, *46*, 1002–1018.

Turco, R. P., et al. (1990), Climate and smoke: An appraisal of nuclear winter, *Science*, *247*, 166–168.

Twitty, J. T., and J. A. Weinman (1971), Radiative properties of carbonaceous aerosols, *J. Appl. Meteorol.*, *10*, 725–731.

D. Baumgardner and G. Raga, Centro de Ciencias de la Atmósfera, Universidad Nacional Autónoma de México, Mexico City, 04510, Mexico. (darrel@servidor.unam.mx)

G. Kok, Droplet Measurement Technologies, Boulder, CO 80301, USA.